JOURNAL OF MULTIFUNCTIONAL MATERIALS & PHOTOSCIENCE
5(2), December 2014, pp. 109-131

Photodegradation of 4-chlorophenol on hybrid TiO_2-C Materials

J. Matos*

[a]*Dpt. Photocatalysis and Alternative Energies, Venezuelan Institute for Scientific Research (IVIC), 20632 Caracas 1020-A, Venezuela*

Abstract: This work reviews the associative effects found between TiO_2 and activated carbon (AC) in the photocatalytic degradation of 4-chlorophenol (4CP). Results are presented in terms of the photoactivity to disappearance of the pollutant and to the photoselectivity for the intermediate products detected. The results showed a clear correlation between photocatalytic activity of TiO_2 with texture and surface chemistry of carbons. The addition of basic AC to TiO_2 under UV irradiation induces a beneficial effect on the photocatalytic degradation of 4CP, quantified by the apparent first-order rate constant up to about 3 times higher in the photoefficiency of the photocatalyst, suggesting that is possible to obtain clean water in a much shorter time than with TiO_2 alone. This effect has been explained by an important adsorption of the pollutants on AC followed by a mass transfer to photoactive Titania through a common interface between AC and TiO_2. Significant differences in the intermediate product distributions were observed and ascribed to the characteristics of each AC, as a consequence of different mechanism of adsorption of the molecule and to different oxidation mechanisms.

Keywords: Photocatalysis, TiO_2, activated carbon, 4-chlorophenol.

1. Introduction

Traditionally, pollution has a direct relationship with increasing and the growing of the population, which demands ever increasing quantities of energy and the manufacture of goods by processing which yield by-products that require removal to some kind of sink, the earth's atmosphere being one of these sinks [1]. It is indeed difficult to separate air and water pollution. The winds contribute both to the spread and, in some instances, to the contributions of air pollutants. Frequently, as in the case of acid rain, the precipitation of water in the form of rain, snow, sleet, ice pellets, etc; causes entrainment of pollutants (gases, particles, etc). Thus, the soils, rocks, lakes and rivers are subject to the corrosive and bio destructive processes brought about by the presence of alien substances [1]. Water, pre-requisite for life and key resource of humanity, is abundant on earth. However, 97.5% is salt water. Of the remaining 2.5% that is fresh water, 70% is frozen in the polar icecaps; the rest is mainly present as soil moisture or in inaccessible subterranean aquifers. Only

*Corresponding author: *jmatos@ivic.gob.ve, jmatoslale@gmail.com*

less than 1% of the world's fresh water resources are readily available for human use; and even this resource is very unevenly distributed [2]. On the ''blue planet'' nearly 1000 million people still have no access to adequate water sources, and about 2400 million have no access to adequate sanitation. Different organic compounds are commonly found in contaminated water. Among these, phenols and molecules that contain phenolic groups are relatively frequent as contaminants [3]. During the last few decades, the total amount of pollutants in the atmosphere has increased exponentially. Even though many of these substances are measured of a scale of parts per million (ppm) or even parts per billion (ppb), a majority of these substances cause ill effects on the health and well-being of air-breathing creatures as well as corroding and eroding structures. As a consequence, 2.2 million people in developing countries, most of them children, die every year from diseases associated with a lack of safe drinking water, inadequate sanitation and poor hygiene [4,5].

Pollutants removal may only involve techniques adopted in governmental regulations, such as flocculation, filtration, sterilization, and conservation procedures to which have been added chemical treatment techniques involving a limited numbers of chemicals, mostly stable precursors for hydroxyl radical production [6]. Recent developments in the domain of chemical water and air treatment have led to an improvement in oxidative degradation procedures for organic compounds dissolved or dispersed in aquatic and air media, in applying catalytic and photochemical methods. They are generally referred to as advanced oxidation processes (AOP´s) [6,7]. The need for highly efficient new methods for the treatment of toxic and biologically persistent compounds has led to a compelling interest in semiconductor-mediated photooxidative degradation [7]. Heterogeneous photocatalysis has emerged as an efficient method for purifying water and air [6,8-11] in most of the cases encountered. This discipline includes a large variety of reactions: mild or total oxidations, dehydrogenation, hydrogen transfer, metal deposition, water detoxification, gaseous pollutant removal and so on. In line with the principles of green chemistry, the heterogeneous photocatalysis can be considered as one of the new AOP´s for air and water purification treatment [12]. This technique utilizing titanium dioxide (TiO_2) has been increasing popularity for the environmental treatment and purification purposes [13]. TiO_2 is non-expensive, non-toxic, and biocompatible material that shows high photoefficiency. This material is the most photoactive catalyst because of its peculiar aptitude of combining good adsorptive properties with respect to diluted pollutants with good absorptive properties with respect to near UV photons.

Several attempts have been made to increase the photoefficiency of TiO_2, either by noble metal deposition [14] or by ion doping [14,15], but such modifications did not enhance its photocatalytic activity and were rather detrimental. A third way to possibly increase the photocatalytic efficiency of TiO_2 consists of adding a co-adsorbent such as silica, alumina, zeolites, and so on [6-18], but not improvement of photoefficiency was observed. Activated Carbon (AC) is another type of co-adsorbent that has been used either in gas phase or in aqueous phase in the photodegradation of organics pollutant [19-29]. Already, a synergy effect has been observed when using powdered TiO_2 and a powdered AC in the photocatalytic degradation of model pollutants [20-23]. Remarkable different effects were

observed in the kinetics of disappearance of the pollutants as well as in the kinetics of appearance and disappearance of the intermediate products detected for the different molecules studied in such works. The synergy or inhibition effects and the formation of the different intermediate products detected have been correlated to the origins and the properties of the AC. However, a fundamental general question arises: what are the driving forces that modify the photoefficiency of the TiO_2 when it is in contact with AC?. Thus, the main objective of this review is to show any associative or synergistic effects between TiO_2 and activated carbon in heterogeneous photocatalytic degradation of a model pollutant such as 4-chlorophenol, in terms of the photoactivity and photoselectivity of the intermediates products detected.

2. Experimental

2.1. Materials and Synthesis of Activated Carbons

4-chlorophenol (4CP) were purchased from Aldrich, with the highest purity grade and used as received. The main possible intermediate compounds such as hydroquinone (HQ), benzoquinone (BQ), 4-chlorocathecol (4CT) were purchased from Riedel de Haën, Fluka and Aldrich, respectively. The photocatalyst was TiO_2 Degussa P 25, mainly anatase ca. 80% under the shape of non-porous polyhedral particles of ca. 30 nm mean size with a surface area of about $55 m^2.g^{-1}$. Activated carbons (AC) were prepared from sawdust of Algarroba (*Tabebuia Pentaphyla)* wood by two methods. Physical activation under CO_2 flow and pyrolysis under N_2 flow were performed from 450 up to 1000°C by 1h. These AC were denoted $AC_{CO2\text{-}i}$ and $AC_{N2\text{-}i}$, being i activation temperature. Chemical activation was also performed after impregnation of the carbon precursor with different concentrations of $ZnCl_2$, H_3PO_4 and KOH followed by activation under N_2 flow at 450°C by 1h. These carbons were denoted as $AC_{ZnCl2\text{-}i\%}$, $AC_{H3PO4\text{-}i\%}$ and $AC_{KOH\text{-}i\%}$ being i% concentration of $ZnCl_2$, H_3PO_4 and KOH, respectively.

2.2. Photoreactor and Procedure

Experiments were carried out in a batch photoreactor showed in Figure 1. It consist of a cylindrical flask made of Pyrex of ca. 60 mL open to air, with an integrated water-circulating jacket (20°C) of about 6 cm diameter. Its optical Pyrex window (at the bottom) of about 3 cm in diameter was mounted at a distance of 6 cm from the top of the lamp assembly, which consisted of a horizontal HPK 125 W mercury lamp supplied by Phillips, fixed in the middle of a vertical metallic cylinder cooled by water circulation. The system was working in a pure photocatalytic regime since the irradiation spectrum was cut-off 335 nm using a Corning 0-52 filter eliminating shorter wavelengths able to induce side photochemical reactions. After maintained in the dark during 80 min to reach a complete adsorption at equilibrium the photocatalytic test were performed at room temperature (20°C) using 50 mg TiO_2 and 10 mg AC under stirring in 25 mL of a millimolar solution of 4CP (about 100 ppm). The quantity of 50 mg of titania was chosen since in our conditions there is a full absorption of the UV light (photon flux about 2.92×10^{15} photons.$cm^{-2}.s^{-1}$) entering the photoreactor in such quantity of semiconductor. The quantity of 10 mg AC

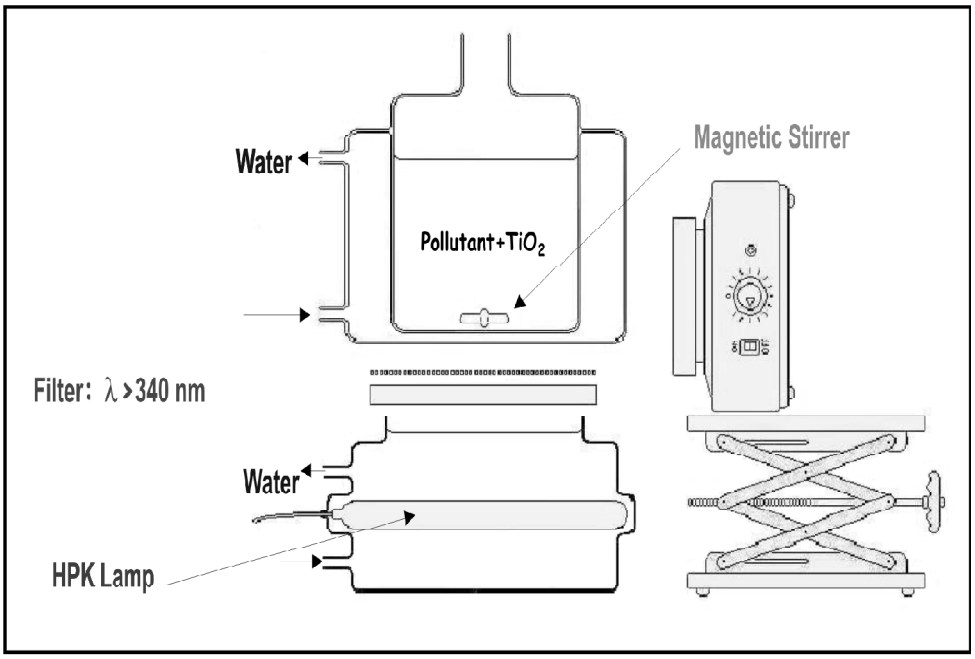

Figure 1: Experimental photochemical reactor in aqueous phase.

was chosen to ensure a good adsorption of 4CP related to the surface area of AC without disturbing the UV absorption of photons by TiO_2 [20-22]. It has been previously shown that stirring the suspension in air provided enough oxygen for the oxidative degradation (≤ 1.4 mmol.L^{-1}) [12]. Samples (0.3 mL) were removed of the suspension at regular's intervals for analysis and Millipore disks (0.45 mm) were used to remove particulate matter before HPLC analysis in a Varian 9010 series HPLC systems equipped with a Spectra Systems UV 2000 absorbance detector adjusted at 280nm.

2.3. Characterization of Activated Carbons

The nature of the acid and basic surface sites in AC were determined by measurement of pH of the point zero charge (pH_{PZC}) [30]. This parameter was measured by the so-called pH drift method [31-32]. For this purpose, 5 mL of a 0.01 M NaCl solution was placed at room temperature, and the pH was then adjusted to successive initial values between 2 and 10, by adding either HCl (0.1 and 0.01 M) or NaOH (0.1 and 0.01 M) and activated carbon (15mg) was added to the solution the final pH, reached after 48 h, was measured and plotted against the initial pH. The pH at which the curve crosses the line $pH_{final} = pH_{initial}$ is taken as the pH_{PZC} of the given carbon. BET surface area (S_{BET}) was estimated from the full isotherms of N_2 adsorption in the range of 0.03 up to 630Torr in a Micromeritics ASAP-2010 apparatus. A summary of the surface pH (pH_{PZC}) and BET surface area (S_{BET}) of the materials presented in this review are showed in Table 1 and Table 2. The hybrid materials were obtained by mixing TiO_2 with AC at the same work conditions in 5mL of water continuously stirred for 80 min. After this, the mixture was filtered and dry around

Table 1
BET Surface Areas (S_{BET}) and Surface pH (pH_{PZC}) of AC Prepared by Physical Activation and Pyrolysis

System	$S_{BET}(m^2/g)$	pH_{PZC} [a]	*System*	$S_{BET}(m^2/g)$	pH_{PZC} [a]
TiO_2	50 ± 2	6.5	$AC_{N2\text{-}1000}$	518 ± 17	8.9
$AC_{CO2\text{-}900}$	548 ± 21	9.1	$AC_{N2\text{-}900}$	590 ± 17	8.5
$AC_{CO2\text{-}800}$	770 ± 16	8.5	$AC_{N2\text{-}800}$	519 ± 15	8.0
$AC_{CO2\text{-}700}$	570 ± 14	8.0	$AC_{N2\text{-}700}$	388 ± 13	7.9
$AC_{CO2\text{-}600}$	426 ± 13	7.2	$AC_{N2\text{-}600}$	360 ± 12	7.1
$AC_{CO2\text{-}450}$	352 ± 5	6.3	$AC_{N2\text{-}450}$	31 ± 5	6.1

[a] pH_{PZC} with less than 5% of standard deviation

Table 2
BET Surface Areas (S_{BET}) and Surface pH (pH_{PZC}) of AC Prepared by Chemical Activation

System	$S_{BET}(m^2/g)$	pH_{PZC} [a]	*System*	$S_{BET}(m^2/g)$	pH_{PZC} [a]	*System*	$S_{BET}(m^2/g)$	pH_{PZC} [a]
$AC_{ZnCl2\text{-}65}$	2001 ± 60	4.5	$AC\text{-}_{H3PO4\text{-}65}$	1569 ± 47	3.1	$AC_{KOH\text{-}65}$	309 ± 15	6.1
$AC_{ZnCl2\text{-}35}$	2485 ± 75	4.8	$AC_{H3PO4\text{-}35}$	1987 ± 60	3.5	$AC_{KOH\text{-}50}$	476 ± 14	6.5
$AC_{ZnCl2\text{-}5}$	561 ± 17	6.0	$AC_{H3PO4\text{-}5}$	414 ± 12	4.0	$AC_{KOH\text{-}5}$	17 ± 1	7.5
$AC_{ZnCl2\text{-}1}$	30 ± 1	6.4	$AC_{H3PO4\text{-}1}$	188 ± 6	4.7	$AC_{KOH\text{-}1}$	5.2 ± 0.2	7.7

[a] pH_{PZC} with less than 5% of standard deviation

12 hours. Scanning electronic microscopy (SEM) was used to verify morphological changes of TiO_2 in the TiO_2-AC and determine the magnitude of common interface between both solids phase. The experiments of SEM were performed on palladium-gold-coated samples using a Hitachi apparatus model S-800.

3. Results

3.1. Preliminary Studies

3.1.1. Degradation Kinetic Order

The kinetic orders of the 4CP disappearance on UV-irradiated TiO_2 and TiO_2-AC were determined using the tangential method. For that, a series of experiments were carried out at different initial concentrations under a constant photon flux (2.92×10^{15} photons. cm^{-2}. s^{-1}). The photocatalytic degradation rate *r* of the 4CP can be expressed as a function of concentration at equilibrium adsorption according to equation (1).

$$r = \frac{-dC}{dt} = k_{app}.C_{eq}^{\ \alpha} \quad (1)$$

where k_{app} is the apparent rate constant. The log-log plot, $r = f(C_{eq})$ gives a straight line ($\log r = \log k_{app} + \alpha \log C_{eq}$) of which slope is equal to the kinetic order. Figure 2 shows the log-log diagrams obtained with two different behaviors. Under UV-irradiated TiO_2 alone, the slope of disappearance of 4CP is $\alpha = 1/2$ indicating the reaction followed half-order kinetics according to the equation (2).

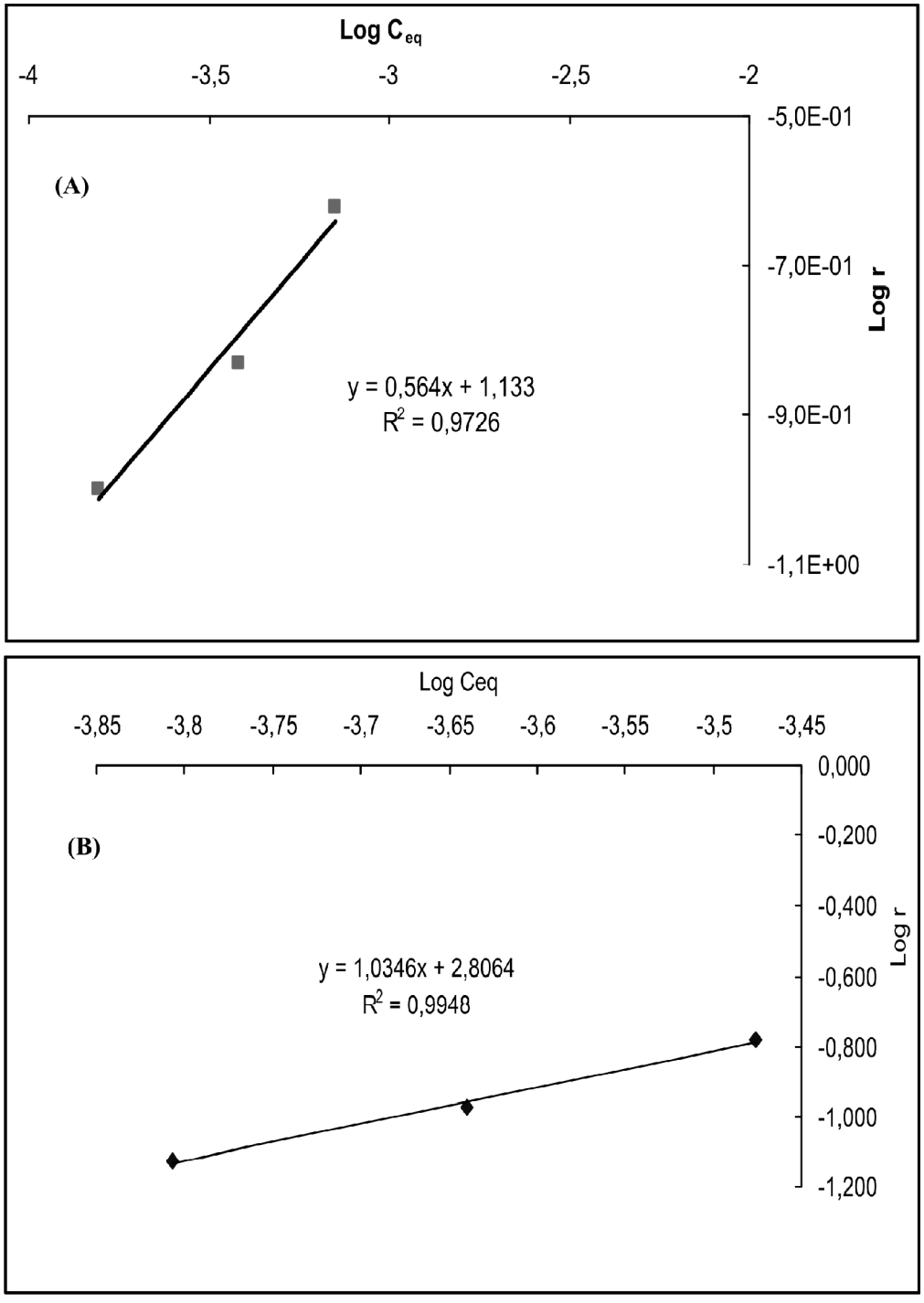

Figure 2: Log-log of the initial rate of photocatalytic degradation of 4CP as a function of concentration at equilibrium adsorption. (A): TiO_2. (B): TiO_2-AC

$$\frac{-dC}{dt} = k_{ap}\sqrt{C}_{eq} \quad (2)$$

By contrast, in presence of a selected AC with basic surface pH, the slope obtained on the irradiated binary material TiO_2-AC is equal to unity ($\alpha = 1$) indicating the reaction followed a first-order kinetic law, according to the equation (3).

$$\frac{-dC}{dt} = k_{ap}C_{eq} \quad (3)$$

First-order kinetics suggests a catalytic reaction with an associative adsorption of the reactant, whereas half-order kinetics suggests a dissociative adsorption [33-34]. The two types of adsorption (associative and dissociative) can co-exist on TiO_2 surface. The half-order kinetic found could indicate that 4CP react under irradiated TiO_2 in the dissociative state. By contrast, the hybrid TiO_2-AC does not follow a half-order kinetic law suggesting 4CP is adsorbed in the neutral form. These results seem to indicate that changes in the distribution of the main intermediate products should be expected as discussed below.

3.1.2. Adsorption of 4-chlorophenol

The study of 4-chlorophenol adsorption in the dark has been performed at 20°C on neat titania (50 mg), on AC (10 mg) and on a suspended mixture of both solids with the same respective weights. The kinetic of adsorption in the dark was followed during 80min under stirring for different initial concentrations between $0.7x10^{-4}$ and $0.7x10^{-2}$ $mol.L^{-1}$. The kinetics of adsorption for the initial 4CP concentration $C_o = 0.7x10^{-4}$ $mol.L^{-1}$ are given in Figure 3. The 4CP adsorbed in the dark on the different samples of the present review are given in Table 3 and Table 4. It can be seen from Fig. 3 that most of adsorption occurred within 20 min and also that 4CP adsorbed on TiO_2-AC is slightly higher than on pure AC. By comparison of values of 4CP adsorption in table 3 and Table 4, it can be inferred that not total additive of the adsorption capacities of both solids were found when they are mixed. This result can be ascribed to a strong interaction between TiO_2 nanoparticles and AC which creates an intimate interface non accessible to 4CP molecules from the solution. Adsorption characteristics of AC are determined by its porous framework (surface area and pore size distribution) and surface chemistry (type of heteroatoms and nature of chemical function) discussed below. However, it can be introduce the fact that the existence of different functional groups such as carboxylates, phenols, lactones, aldehydes, ketones, quinones, hydroquinones and anhydrides has been reported [35]. These groups determine the acid-base character of AC and they derive either from the precursor or may be introduced by additional treatment. The electrical change of the surface groups may also enhance or decrease the adsorption of the target molecules on the carbon surface. If the adsorbate has the same electrostatic charge as that of the carbon surface, repulsion occurs, this lead to decrease in adsorption. However, if adsorbate and the carbon surface show opposite charges, adsorption increases. In this sense, the adsorption isotherms $n_{ads} = f(C_{eq})$ was determined by assuming the conventional Langmuir isotherm model with a surface coverage q varying as indicate equation 4.

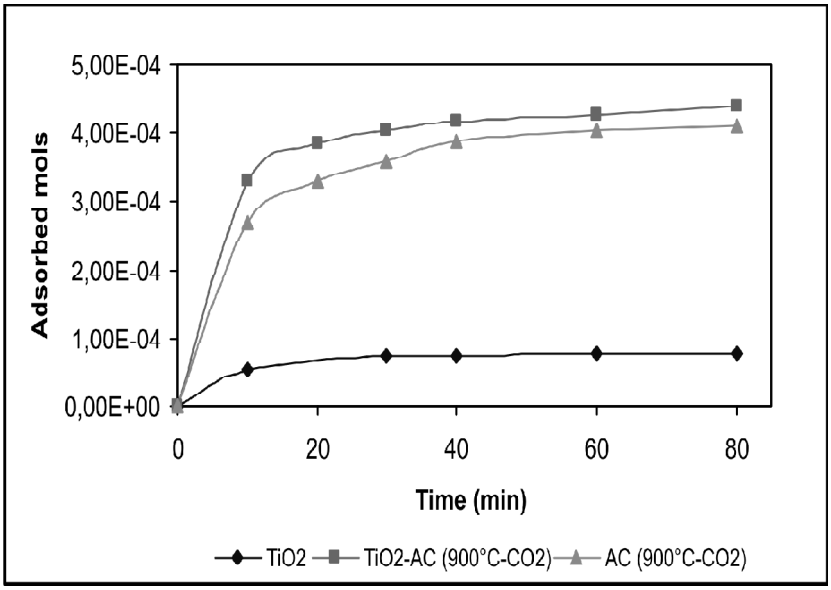

Figure 3: Adsorbed 4CP in the dark. C_o= 0.7x10^{-3}mol.L^{-1}. AC (10 mg), TiO_2 (50 mg) and TiO_2-AC (50mg/10mg)

Table 3
Adsorption in the Dark of 4CP on TiO_2, AC, and TiO_2-AC Prepared by Physical Activation and Pyrolysis

System	*% Adsorbed*[a]
TiO_2	9.8
$AC_{CO2\text{-}900}$	52.1
$AC_{CO2\text{-}800}$	45.0
$AC_{CO2\text{-}700}$	9.0
$AC_{CO2\text{-}600}$	4.8
$AC_{CO2\text{-}450}$	2.8
TiO_2-$AC_{CO2\text{-}900}$	55.8
TiO_2-$AC_{CO2\text{-}800}$	45.00
TiO_2-$AC_{CO2\text{-}700}$	13.8
TiO_2-$AC_{CO2\text{-}600}$	7.6
TiO_2-$AC_{CO2\text{-}450}$	5.8
$AC_{N2\text{-}1000}$	20.8
$AC_{N2\text{-}900}$	17.7
$AC_{N2\text{-}800}$	17.5
$AC_{N2\text{-}700}$	4.7
$AC_{N2\text{-}600}$	3.7
$AC_{N2\text{-}450}$	3.5
TiO_2-$AC_{N2\text{-}1000}$	23.8
TiO_2-$AC_{N2\text{-}900}$	20.8
TiO_2-$AC_{N2\text{-}800}$	22.0
TiO_2-$AC_{N2\text{-}700}$	6.8
TiO_2-$AC_{N2\text{-}600}$	5.8
TiO_2-$AC_{N2\text{-}450}$	4.9

[a] Values adsorbed in the equilibrium after 80min

Table 4
Adsorption in the Dark of 4CP on TiO_2, AC, and TiO_2-AC Prepared by Chemical Activation

System	*% Adsorbed* [a]
TiO_2	9.8
$AC_{ZnCl2-65}$	51.1
$AC_{ZnCl2-35}$	61.6
$AC_{ZnCl2-5}$	41.3
$AC_{ZnCl2-1}$	2.1
TiO_2-$AC_{ZnCl2-65}$	48.4
TiO_2-$AC_{ZnCl2-35}$	61.2
TiO_2-$AC_{ZnCl2-5}$	34.8
TiO_2-$AC_{ZnCl2-1}$	6.5
$AC_{H3PO4-65}$	44.5
$AC_{H3PO4-35}$	46.5
$AC_{H3PO4-5}$	16.3
$AC_{H3PO4-1}$	6.5
TiO_2-$AC_{H3PO4-65}$	44.1
TiO_2-$AC_{H3PO4-35}$	51.5
TiO_2-$AC_{H3PO4-5}$	11.6
TiO_2-$AC_{H3PO4-1}$	10.9
AC_{KOH-65}	33.5
AC_{KOH-50}	25.6
AC_{KOH-5}	8.6
AC_{KOH-1}	7.4
TiO_2-AC_{KOH-65}	32.9
TiO_2-AC_{KOH-50}	27.4
TiO_2-AC_{KOH-5}	13.0
TiO_2-AC_{KOH-1}	5.7

[a] Values adsorbed in the equilibrium after 80min

$$\theta = \left(\frac{n_{ads}}{n_T} \right) = \left\{ \frac{K_{ads}.C_{eq}}{\left(1 - K_{ads}.C_{eq}\right)} \right\} \quad (4)$$

The Langmuir´s adsoption parameters such as total number of adsorption sites n_T and the adsorption constants K_{ads} were obtained from the linear transform $(1/n_{ads})=f(1/C_{eq})$, with correlation coefficients close to 0.99. The corresponding values are given in Table 5 and Table 6 for the two types of hybrid TiO_2-AC materials. None additive effect in adsorption capacities of both solids were observed in all materials presented in this work suggesting a strong interaction between semiconductor nanoparticles and activated carbon and therefore an important competition between Titania and carbons for the adsorption of the pollutant. In other words, this fact could be interpreted as the creation of an intimate interface between both solids non-accessible to 4CP molecules from the solution.

3.2. Photodegradation of 4CP on TiO_2 and AC_{CO2} and AC_{N2}

3.2.1. Kinetics of 4CP Photocatalytic Disappearance

An example of the kinetics of 4CP photocatalytic disappearance is presented in Fig. 4. It can be observed that the direct photolysis without solids is neglected with less than 8% of conversion within 6 h of UV-irradiation. Similarly, the decomposition of 4CP in presence of UV-irradiated AC prepared by physically activation or by pyrolysis is quite negligible, with less than 2% of conversion after 1 h illumination. Pure titania gives a complete disappearance of 4CP in about 30 h of UV-irradiation. The behaviors of the irradiated mixtures TiO_2-AC were different. The apparent rate constant has been chosen as the basic kinetic parameter to compare the different systems, since is independent of the

Table 5
Adsorption Constant (K_{ads}) and Total Number of Adsorption Sites (n_T) for 4CP on TiO_2, AC and TiO_2-AC Prepared by Physical Activation and Pyrolysis

Solids	K_{ads} *(L.mol-1)*	n_T *(mol)* $x10^{-5}$
TiO_2	136	1.55
$AC_{CO2-900}$	2715	2.03
TiO_2-$AC_{CO2-900}$	3100	2.12
$AC_{CO2-800}$	1830	1.98
TiO_2-$AC_{CO2-800}$	1930	1.92
$AC_{CO2-700}$	426	2.10
TiO_2-$AC_{CO2-700}$	362	2.38
$AC_{CO2-600}$	15.5	9.15
TiO_2-$AC_{CO2-600}$	14.7	1.55
$AC_{N2-1000}$	956	1.08
TiO_2-$AC_{N2-1000}$	1390	1.02
AC_{N2-900}	592	1.25
TiO_2-$AC_{N2-1000}$	768	1.18
AC-AC_{N2-800}	643	1.17
TiO_2-AC_{N2-800}	879	1.10

Table 6
Adsorption Constant (K_{ads}) and Total Number of Adsorption Sites (n_T) for 4CP on TiO_2, AC and TiO_2-AC Prepared by Chemical Activation

Solids	K_{ads} *(L.mol^{-1})*	n_T *(mol)*$x10^{-5}$
$AC_{ZnCl2-35}$	1470	3.87
TiO_2-$AC_{ZnCl2-35}$	1440	3.89
$AC_{ZnCl2-5}$	1360	1.86
TiO_2-$AC_{ZnCl2-5}$	1230	2.05
$AC_{H3PO4-35}$	1710	2.65
TiO_2-$AC_{H3PO4-35}$	1640	2.60
$AC_{H3PO4-5}$	519	1.25
TiO_2-$AC_{H3PO4-5}$	424	1.30
AC_{KOH-5}	175	1.52
TiO_2-AC_{KOH-5}	284	1.28

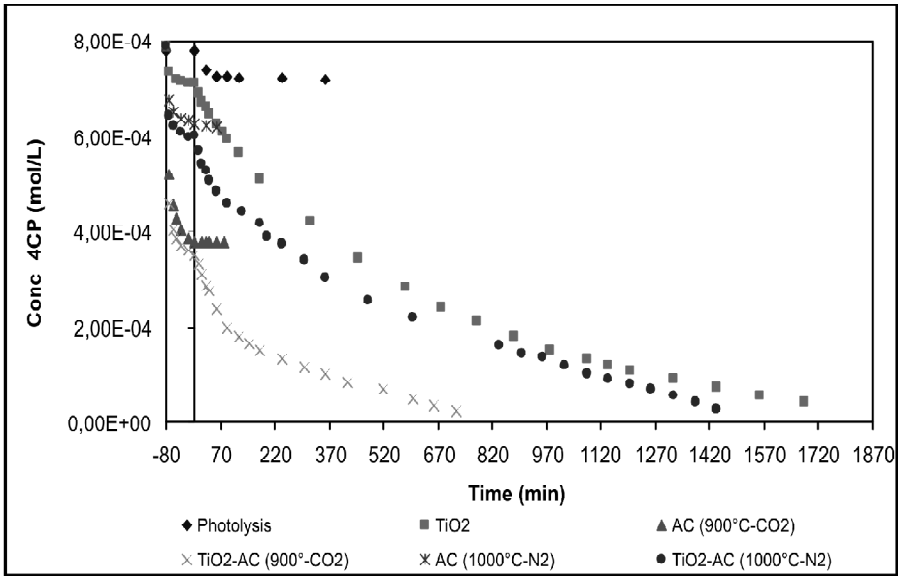

Figure 4: Kinetics of 4CP disappearance under selected AC prepared by physical activation. Vertical line at t = 0, separates the dark period from the UV irradiated one

concentration and therefore enables one to determine the photocatalytic activity independently of the previous adsorption period in the dark. The kinetics curves suggest an apparent first order as confirmed by the linear transforms showed in Fig. 5. Apparent rate constants (k_{app}) were found from the linear regression of equation 5.

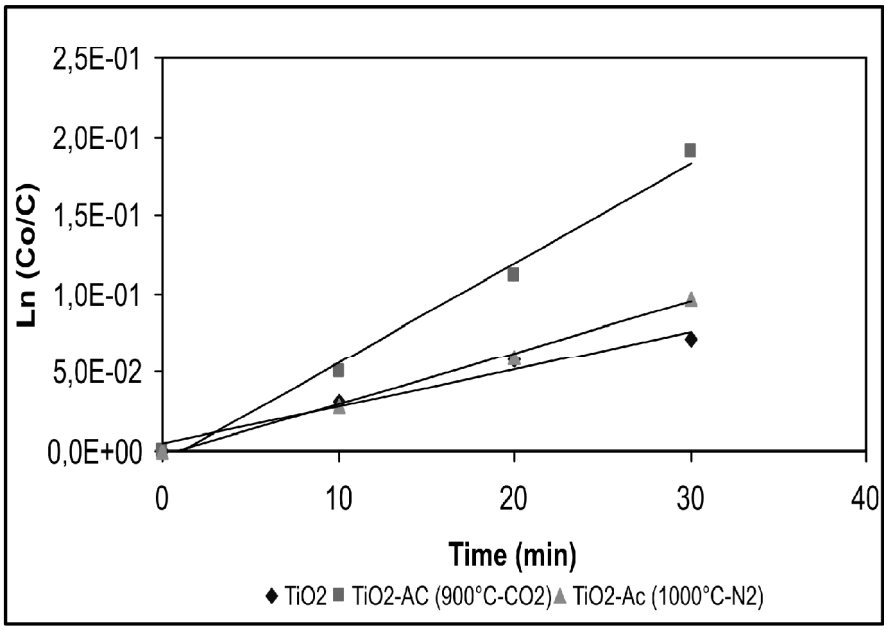

Figure 5: Linear transform Ln (C_o/C_t) = f(t) of the kinetics data from Fig. 4

$$Ln\left(\frac{n_0}{n}\right) = k_{app}.t \quad (5)$$

These values are summarized in Table 7. It can be seen that k_{app} obtained on TiO_2-$AC_{CO2-900}$ and TiO_2-$AC_{N2-1000}$ are high and monotonically decrease when the activation temperature of AC also decreases. In the last column of Table 7 we can observe the ratio between k_{app} obtained on each TiO_2-AC against the k_{app} obtained on neat TiO_2. This ratio defined as the interaction factor (I_F) describes the any associative, synergistic or inhibiting effects between TiO_2 and AC in the photocatalytic disappearance of 4CP. Although the reaction rate is in some cases higher for TiO_2 than for TiO_2-AC because of a higher concentration at time $t_{UV} = 0$, the photocatalytic activity of the hybrid TiO_2-AC determined from the apparent rate constant is higher than that of neat TiO_2. In other words, the photocatalytic activity of TiO_2 with some AC was higher than that of neat TiO_2, indicating a positive associative (synergy) effect with an increase of the rate constant. By contrast, the addition of some AC was found detrimental. The increase in activity cannot be ascribed to an increase of temperature induced by the presence of black AC. It was found that adding 10 mg AC to an UV-irradiated suspension of TiO_2 the increase in the temperature was only of 1°C after 5h irradiation. Since the activation energy for this reaction is about 5 $kJ.mol^{-1}$ [22], the influence of 1°C increase in temperature upon photoactivity of TiO_2 is quite negligible [22]. We observed that the synergy effect between solids increases as function of activation temperature of AC (Fig. 6) as consequence of increase of electronic charge density on TiO_2 due to the interaction with AC. As discussed below, the higher the surface pH of AC the higher the transference of charge density from AC to TiO_2 by means of the contact interface between both solids formed during reaction. In this common contact interface, AC acts as an efficient adsorption trap to the organic pollutant, which is then more efficiently transferred to the TiO_2 surface where it is photocatalytically degraded in shorter irradiation time as suggest the increase in the first-order apparent-rate constants (Table 7).

Table 7
Apparent Rate Constants of the Photodegradation of 4CP on UV-Irradiated TiO_2 and TiO_2-AC Prepared by Physical Activation and Pyrolysis

System	k_{app} $(min^{-1})x10^{-3}$	I_F [a]
TiO_2	2.392	1.0
TiO_2-$AC_{CO2-900}$	6.342	2.7
TiO_2- $AC_{CO2-800}$	5.966	2.5
TiO_2- $AC_{CO2-700}$	4.552	1.9
TiO_2-$AC_{CO2-600}$	2.446	1.0
TiO_2-$AC_{CO2-450}$	2.196	0.9
TiO_2-$AC_{N2-1000}$	4.412	1.8
TiO_2-AC_{N2-900}	3.240	1.4
TiO_2-AC_{N2-800}	1.705	0.7
TiO_2-AC_{N2-700}	1.541	0.6
TiO_2-AC_{N2-600}	0.943	0.4
TiO_2-AC_{N2-450}	0.680	0.3

[a] Interaction factor (I_F) between TiO_2 and AC defined by: $I_F = k_{app(AC\text{-}TiO2)}/k_{app(TiO2)}$

3.2.2. Kinetics of appearance and disappearance of intermediate products on TiO_2 and AC_{CO2} and AC_{N2}

Significant differences in intermediate products distributions were observed. Results are presented in Fig. 7. As expected, hydroquinone (HQ) and benzoquinone (BQ) were the main intermediate products observed in all the samples studied. However, 4-chlorocathecol (4CT) was also detected in some hybrids, but the proportion of this product shown different trends according to the chemical nature of AC employed. In presence of AC prepared at high temperatures, small quantities of 4CT were observed, but this proportion increases when activation temperature of the AC decrease suggesting that chemical nature of AC strongly influence the product distribution indicating that the degradation mechanism can be different.

3.3. Photodegradation of 4CP on TiO_2 and AC_{ZnCl2}, AC_{H3PO4}, AC_{KOH}

3.3.1. Kinetics of 4CP Photocatalytic Disappearance

A representative example is presented in Fig. 8. It can be observed that the decomposition of 4CP in presence of UV-irradiated AC prepare by chemical activation is quite negligible like in the case of AC physically activated. The kinetics showed apparent first-order as confirmed by the linear transforms of equation 5 showed in Fig. 9. A summary of the apparent rate-constants is shown in Table 8. It can be seen from Fig. 10 that k_{app} obtained

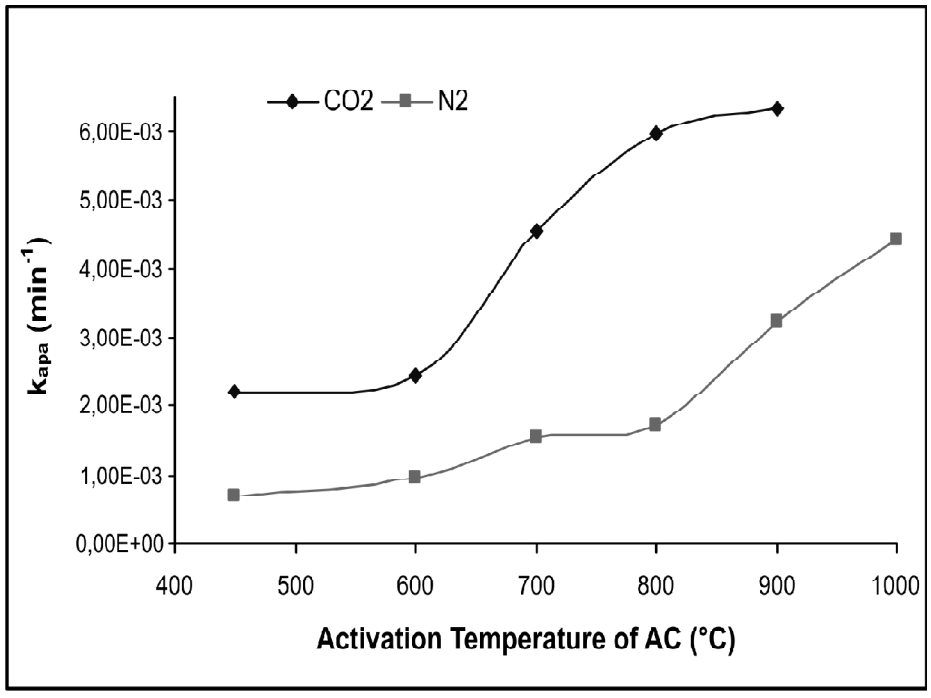

Figure 6: Trends of k_{app} for the 4CP photodegradation on TiO_2 and TiO_2-AC prepared by physical activation and pyrolysis as a function of temperature of activation

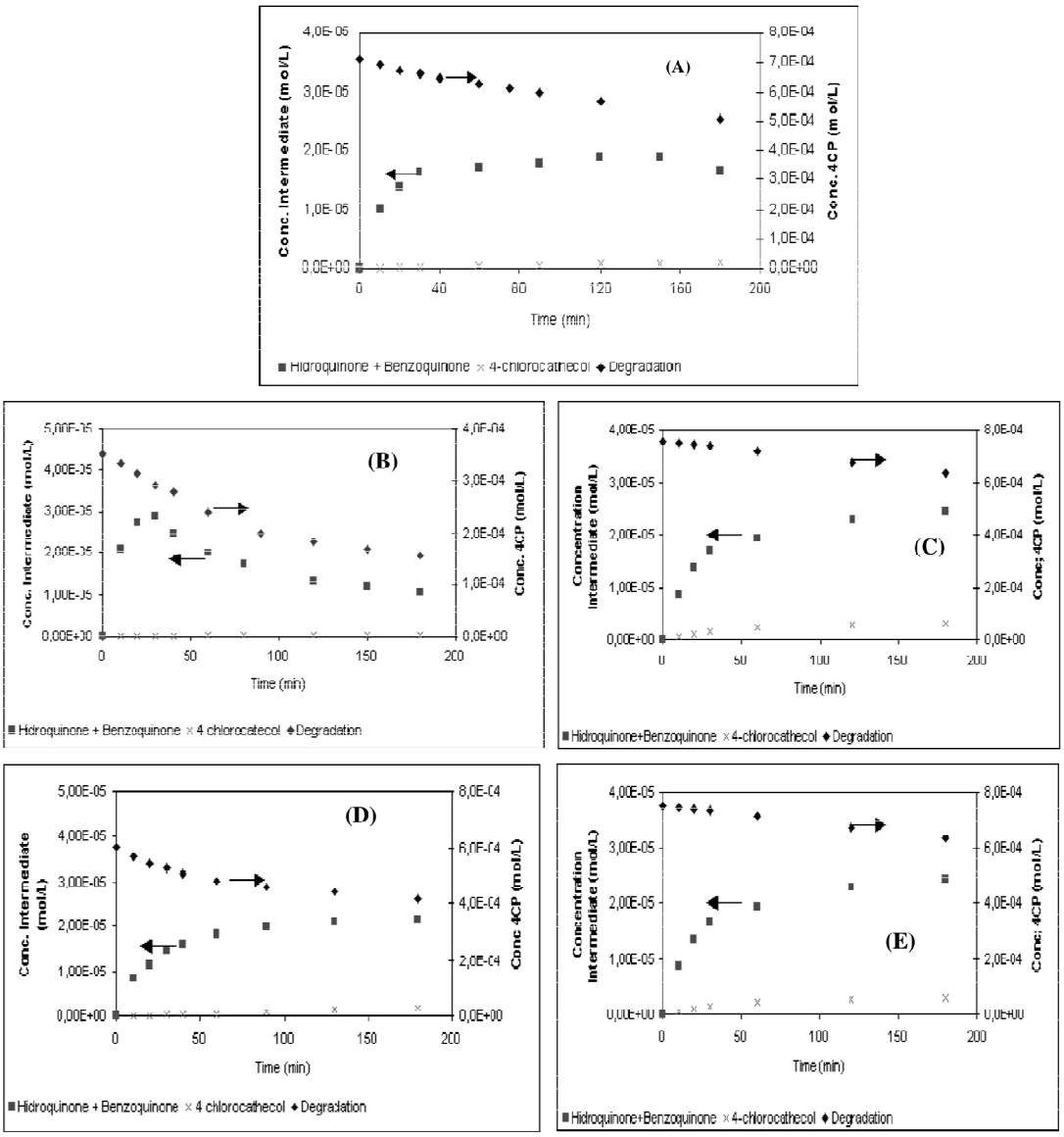

Figure 7: Kinetics of appearance and disappearance of the main intermediate products detected on TiO_2 and TiO_2-AC prepared by physical activation and pyrolysis. (A) TiO_2, (B) TiO_2-$AC_{CO2\text{-}900}$, (C) TiO_2-$AC_{CO2\text{-}450}$, (D) TiO_2-$AC_{N2\text{-}1000}$, (E) TiO_2-$AC_{N2\text{-}1000}$

on TiO_2-AC prepared by chemical activation showed very different trends than those obtained in presence of AC physically activated (Fig. 6). It must be point out that activated carbons prepared with slightly acid concentrations (5% wt. in $ZnCl_2$ and H_3PO_4), shows beneficial effect on the 4CP photodegradation, but this positive influence clearly fall downs when the concentration of acids are increase suggesting a inhibiting role of the acids groups formed on AC upon the TiO_2 photoactivity. By contrast, the curve for ACs with KOH is

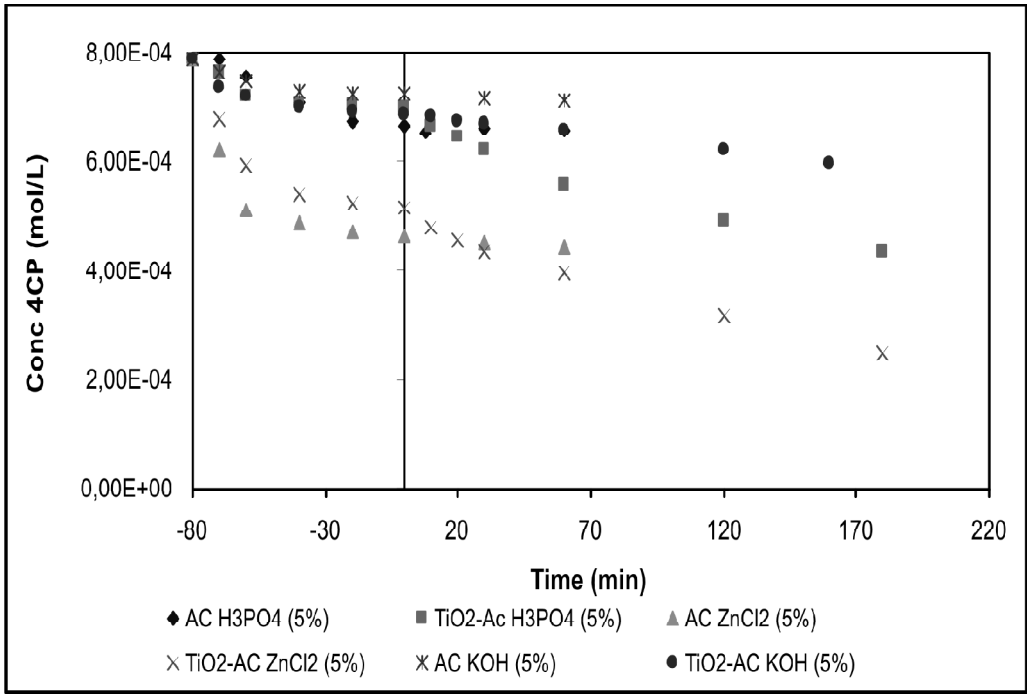

Figure 8: Kinetics of 4CP disappearance under selected AC prepared by chemical activation

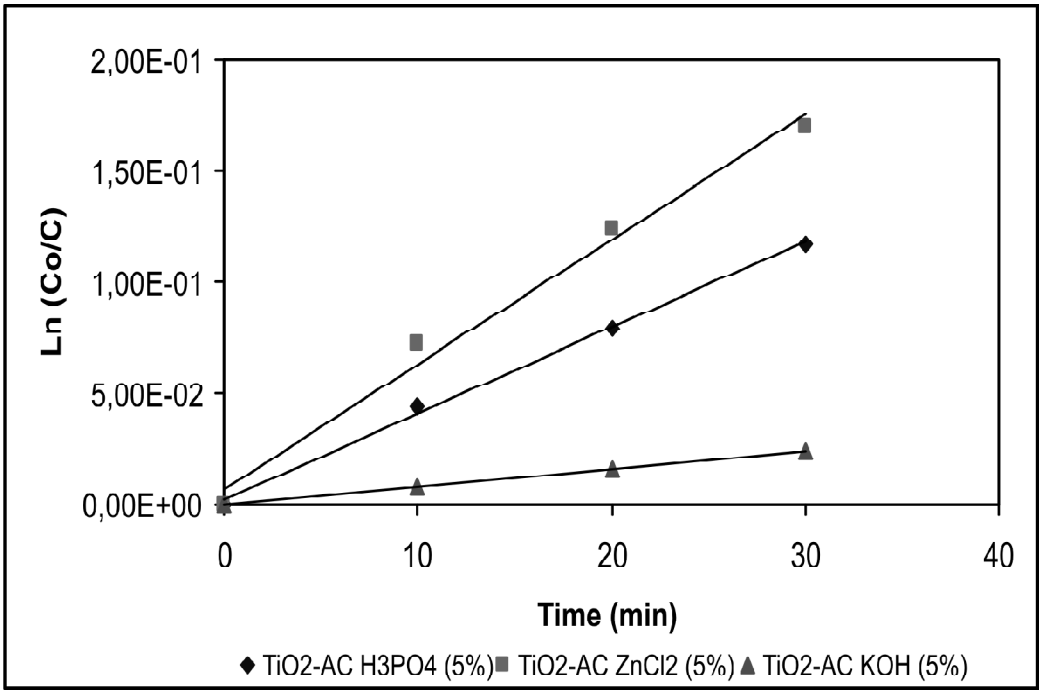

Figure 9: Linear transform Ln (C_o/C_t) = f(t) of the kinetics data from Fig. 8

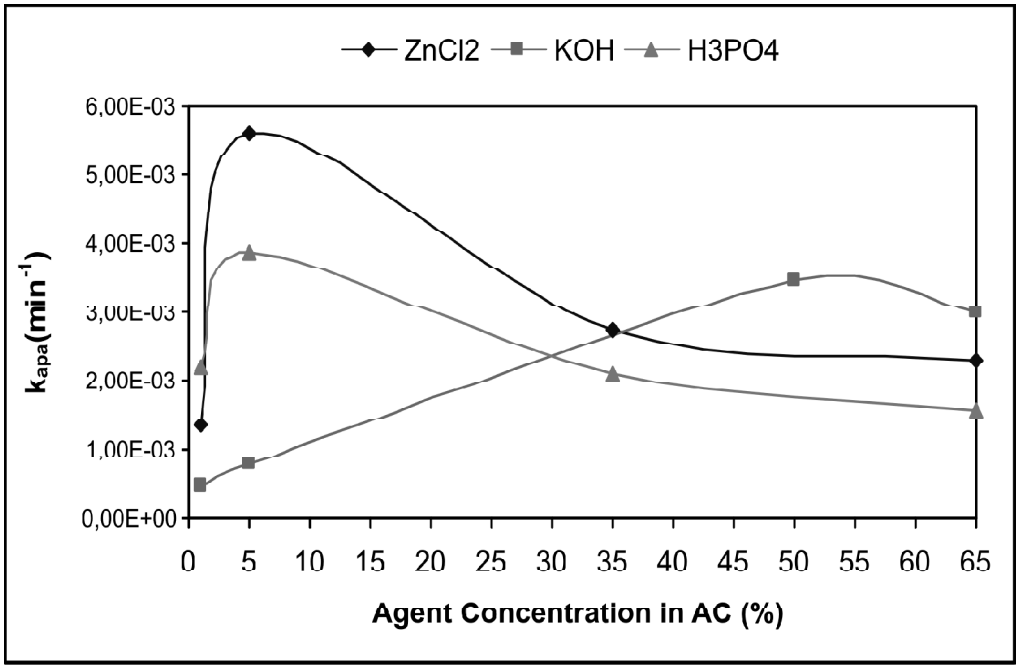

Figure 10: Trends of k_{app} for the 4CP photodegradation on TiO_2 and TiO_2-AC prepared by chemical activation as a function of concentration of chemical activators

Table 8
Apparent Rate Constants of the Photodegradation of 4CP on UV-Irradiated TiO_2 and TiO_2-AC Prepared by Chemical Activation

System	k_{app} $(min^{-1})x10^{-3}$	I_F [a]
TiO_2	2.392	1,0
TiO_2-$AC_{ZnCl2-65}$	2.282	09
TiO_2-$AC_{ZnCl2-35}$	2.727	1.2
TiO_2-$AC_{ZnCl2-5}$	5.603	2.3
TiO_2-$AC_{ZnCl2-1}$	1.344	0.6
TiO_2-$AC_{H3PO4-65}$	1.558	0.7
TiO_2-$AC_{H3PO4-35}$	2.096	0.9
TiO_2-$AC_{H3PO4-5}$	3.875	16
TiO_2-$AC_{H3PO4-1}$	2.210	0.9
TiO_2-AC_{KOH-65}	2.990	1.3
TiO_2-AC_{KOH-50}	3.447	1.4
TiO_2-AC_{KOH-5}	0.800	0.3
TiO_2-AC_{KOH-1}	0.474	0.2

[a] Interaction factor (I_F) between TiO_2 and AC defined by: $I_F = k_{app(AC\text{-}TiO2)}/k_{app(TiO2)}$

significantly different with the highest synergy effect when AC was prepared with 50% KOH.

3.3.2. Kinetics of Appearance and Disappearance of Intermediate Products on TiO_2 and AC_{ZnCl2}, AC_{H3PO4}, AC_{KOH}

Significant changes in the intermediate product distributions were detected as a function of the type of AC added to Ti_{O2}. Results are presented in Fig. 10. As expected, HQ and BQ were the main intermediate products observed. However, important 4CT proportion was found in presence of AC prepared with high concentration of $ZnCl_2$ or H_3PO_4. By contrast, when AC is prepared with small quantities of KOH, only traces of 4CT were observed. Afterwards, the intermediate products distribution is different in each system and depends on the nature of the chemical agent used in AC preparation, indicating that the degradation mechanism is different and is influenced by the chemical nature of the AC. This influence is discussed as follows.

3.4. Influence of Surface Chemistry and Texture of AC upon the Photoactivity of TiO_2

The surface chemistry of carbons materials is determined by the acidic and basic character of the functional groups on their surface [35]. The acidic behavior is associated with oxygen surface complexes or oxygen functionalities such as carboxylates, lactones and phenols. On the other hand, functionalities like pyrones, ethers and carbonyls are responsible for basic properties of the carbon surfaces [36]. However, the chemical properties of the functional groups on carbon surfaces are not fully understood yet. For example, some authors [30, 37-39] have identified basic properties associated with Lewis sites located at the electron p-rich regions within the basal planes of the graphitic microcrystals, away from the edges. Calorimetric measurements [40] suggest that the basic character of carbon surfaces seems to be associated essentially with the absence of oxygen-containing groups with acid nature [39]. Figure 12 shows typical curves of the experimental results obtained with the pH drift method for the estimation of the pH_{PZC}. It can be seen from Table 1 and Table 2 that the surface pH increases when the activation temperature of AC increases. This results are in agreement with the fact that when the carbon precursor is treated at high temperatures the activated carbon develop basic oxygen functional groups [39,40], whereas when low temperature are used then the activated carbons develop acid centers. It can be seen from Fig. 13 the trends developed by the first-order apparent rate-constants obtained on TiO_2-AC as a function of the pH_{PZC} of AC prepared by physical and chemical activation. The differences in the photocatalytic degradation of 4CP on TiO_2 in presence of AC can be attributed mainly to changes in the surface charge of TiO_2 by the interaction with the carbonaceous support during the degradation process. It can be suggested that if carbons increases its surface pH (more basic) the photoactivity of TiO_2 should increases as a consequence of higher electronic density on it.In summary, the higher the activation or pyrolysis temperature the higher the pH_{PZC} which indicate the presence of basic functional groups on the surface of AC and a close topology [41]. A similar trend was observed for S_{BET} where an increase of the thermal treatment leads to an increase of the

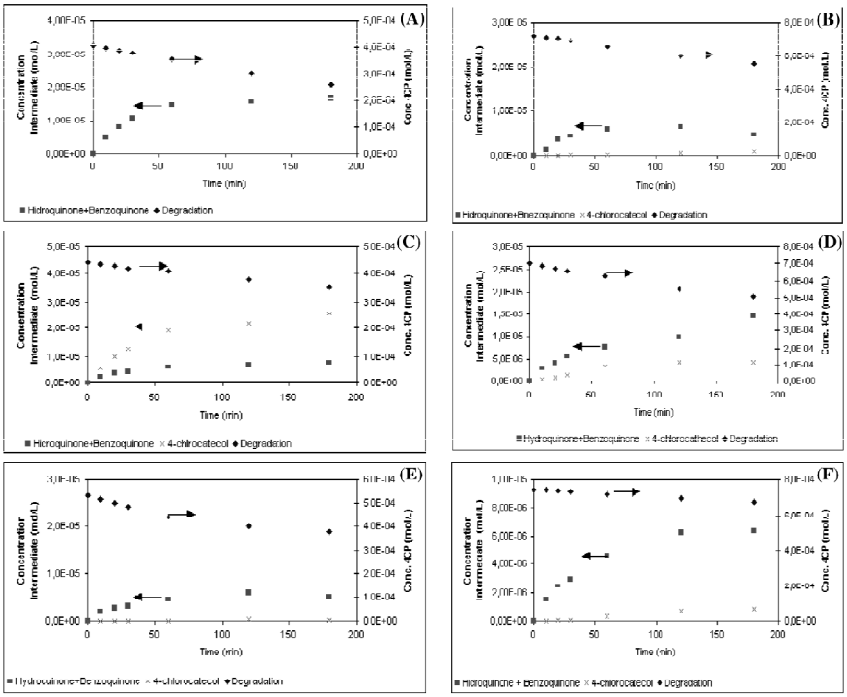

Figure 11: Kinetics of appearance and disappearance of the main intermediate products detected on TiO_2 and TiO_2-AC prepared by chemical activation. (A) TiO_2-$AC_{ZnCl2-65}$, (B) TiO_2-$AC_{ZnCl2-1}$, (C) TiO_2-$AC_{H3PO4-65}$, (D) TiO_2-$AC_{H3PO4-1}$, (E) TiO_2-AC_{KOH-65}, (F) TiO_2-AC_{KOH-1}

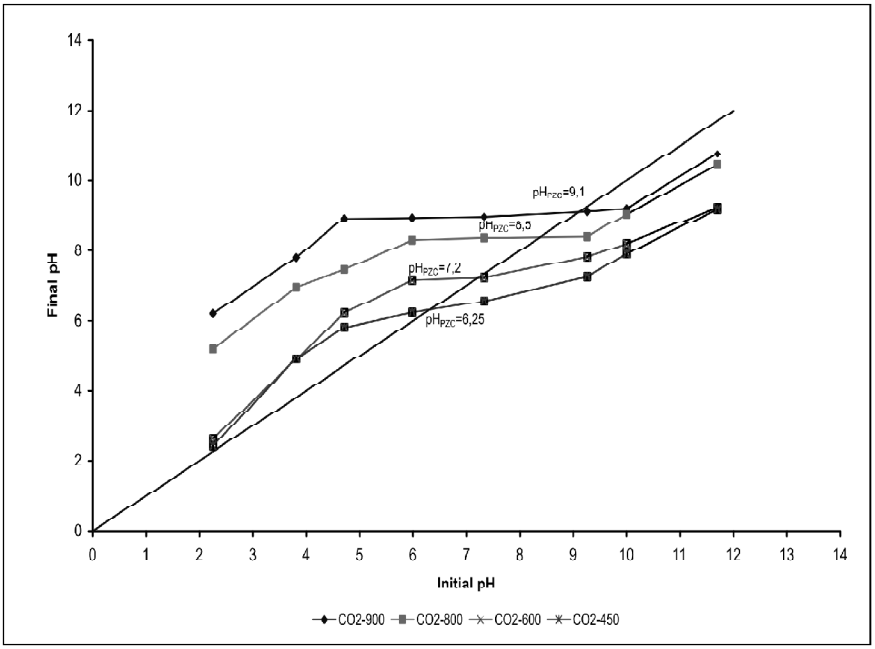

Figure 12: Estimation by drift method of pH_{PZC} of AC prepared by physical activation

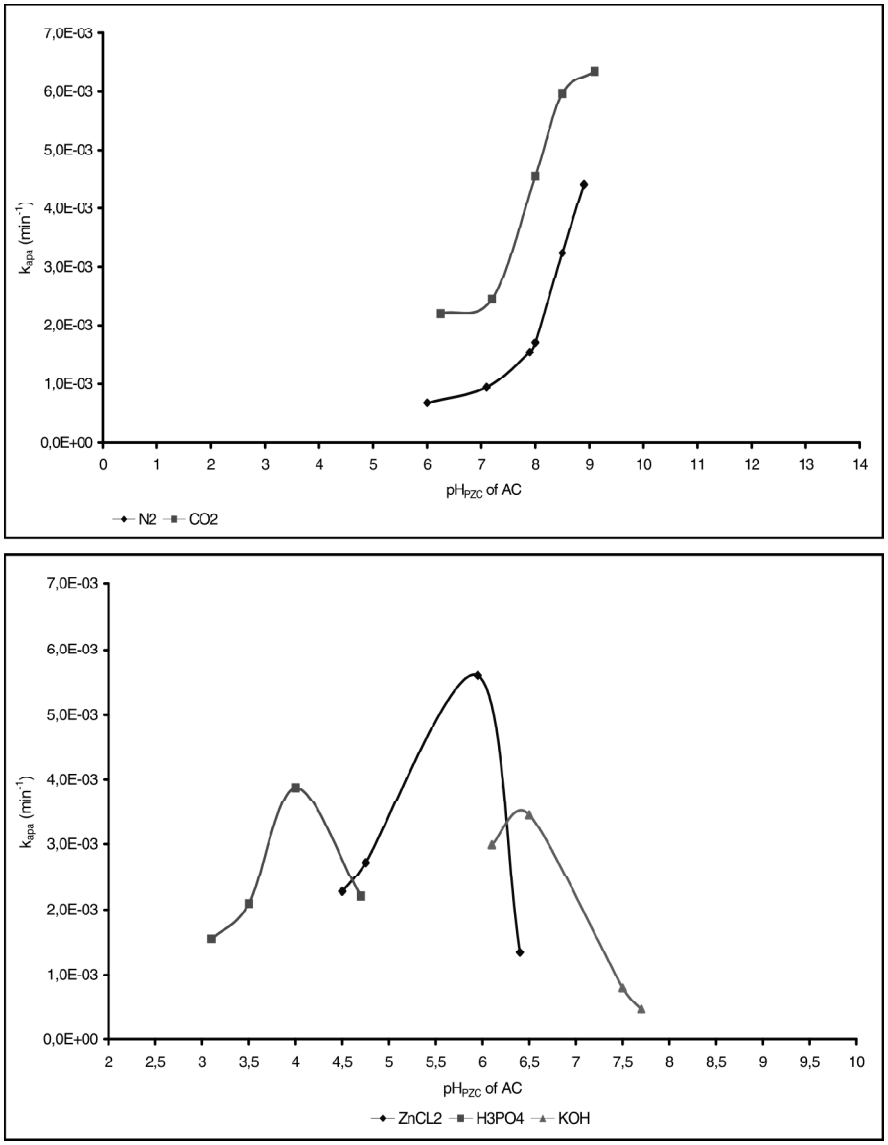

Figure 13: Trends of k_{app} for the 4CP on TiO_2-AC as a function of pH_{PZC}. (A) AC prepared by physical activation. (B) AC prepared by chemical activation

surface areas up to a maximum of 770$m^2.g^{-1}$ around 800°C ($AC_{CO2\text{-}800}$) and of 590$m^2.g^{-1}$ at 900°C ($AC_{N2\text{-}900}$) under CO_2 and N_2 flows, respectively. It is important also to note that if the sawdust from wood is heat at higher temperatures than 800 and 900°C under CO_2 and N_2 flow, respectively, a decrease in S_{BET} was observed. This could be due to excessive gasification by CO_2 or excessive pyrolysis promoted at high temperatures. Concerning to AC prepared by chemical activation, it can be seen from Table 2 that AC prepared with H_3PO_4 showed lower pH_{PZC} values than those AC prepared with $ZnCl_2$. It can be noted from Table 2 that pH_{PZC} of AC prepared with 1%w/w H_3PO_4 is clearly lower than that

obtained for the same concentration of $ZnCl_2$ (4.7 against 6.4). This is the due to H_3PO_4 is a strong Brönsted acid while $ZnCl_2$ is a Lewis acid; therefore, the first one should introduce more positive zeta potential, and our case, more acidic groups on AC surface. Also, it must to be note that AC prepared with KOH showed an apparent unexpected behaviour. Thought KOH is a strong Lewis base, Table 2 show that the higher KOH concentration the lower pH_{PZC} of AC. However, this lowering is only from 7.7 down to 6.1 for the increase of KOH concentration from 1 to 65% w/w. This can be explained by the fact that AC prepared with KOH develops an open topology [41-43] in comparison of $AC_{H\text{-}type}$. On the other hand, it can be seen from Table 2 that the higher the concentration of impregnation compounds the higher S_{BET} areas having a maxima of about 2485, 1987, and 476$m^2.g^{-1}$ for $ZnCl_2$ (35% w/w), H_3PO_4 (35% w/w) and KOH (50% w/w), respectively. It is important to note that employing higher concentrations a clear decrease in S_{BET} is observed. This decrease in S_{BET} has been already reported and in the case of KOH [43] have been explained by a high concentration of steam produced during the thermal decomposition of KOH. In this case, activation would proceeds by a gasification reaction at low temperature: $C + H_2O \rightarrow H_2 + CO$, and due to a higher concentration of steam a decrease in S_{BET} is expected because original microporous texture can be consumed by gasification.

The SEM micrographs of AC prepared by physical and chemical activation are shown in Fig. 14 and Fig. 15, respectively. It can be seen from Fig. 14 that the surface of AC prepared at high temperature are homogeneously covered by TiO_2 nanoparticles. By

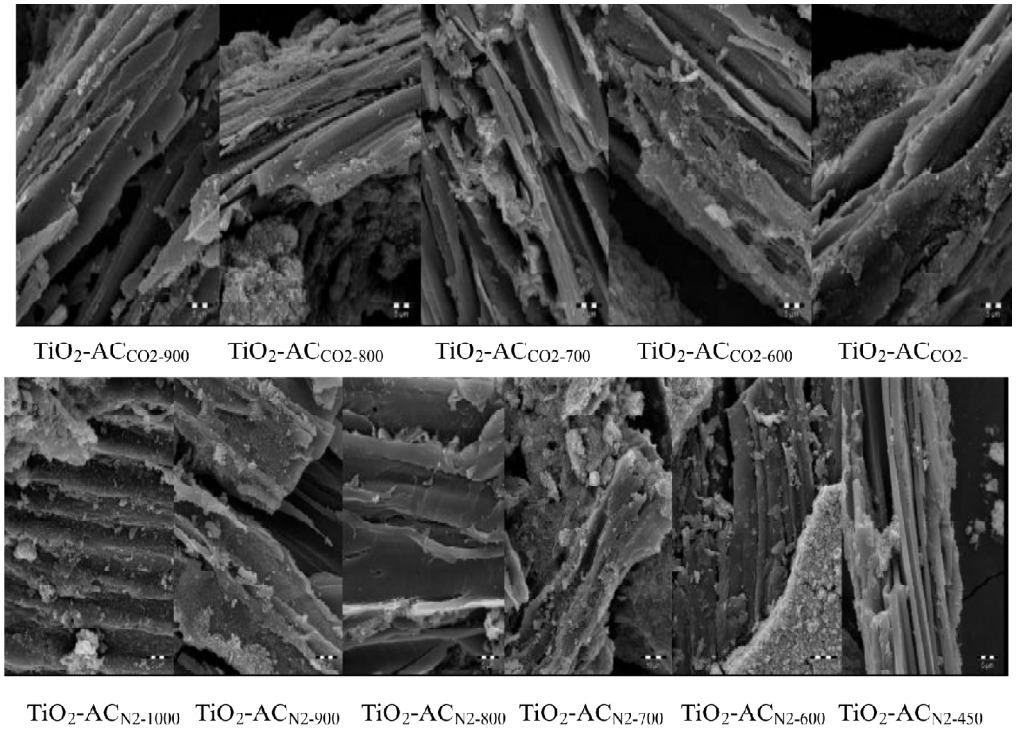

Figure 14: SEM images of TiO_2-AC prepared by physical activation

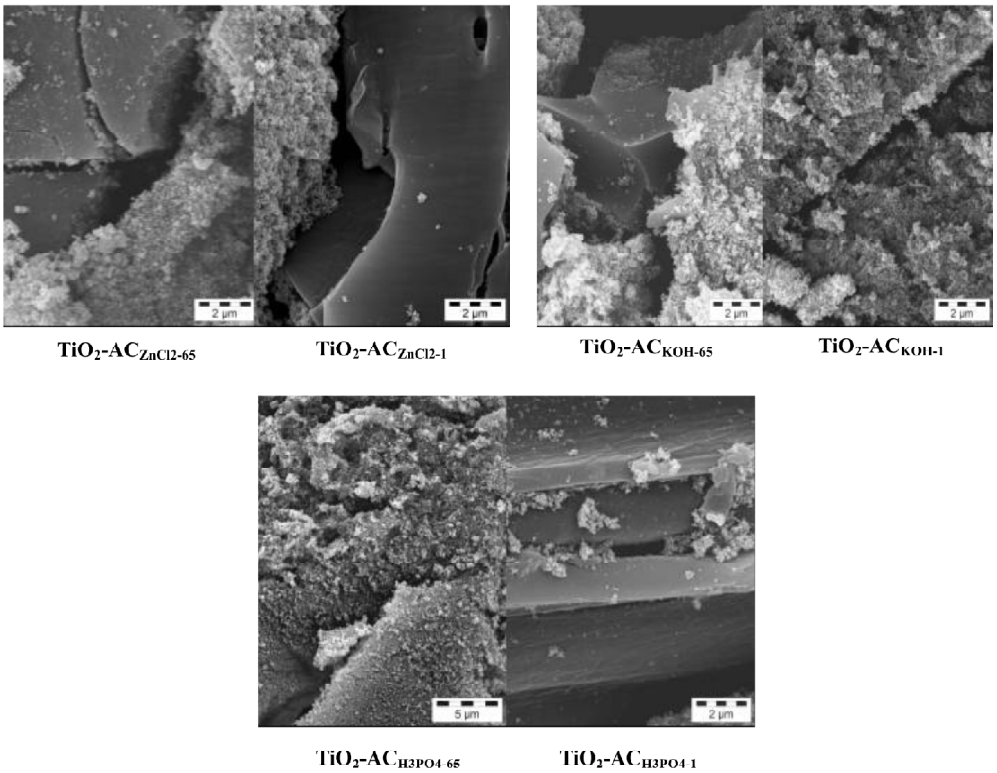

Figure 15: SEM images of TiO_2-AC prepared by chemical activation

contrast, for the case of activated carbons prepared by chemical activation (Fig. 15), large TiO_2 nano-aggregates are formed and surface of carbons are poorly covered by TiO_2. In other words, the contact between solids increases as function of activation temperature and basicity of these materials, and then, the transference of charge density to TiO_2 in promoted by means of contact interface which should be more efficient if the TiO2 nanoparticles are highly dispersed on carbon surface. These differences in the intimate contact between TiO_2 and AC are the key factor for pollutant diffusion and thus enhanced the photodegradation.

4. Conclusions

The present review showed a clear correlation between the photocatalytic activity of TiO_2 and activated carbon properties mainly as a function of texture and surface chemistry of AC. The addition of basic AC to TiO_2 under UV irradiation induces beneficial effects on the photocatalytic degradation of 4CP, quantified by the apparent first-order rate constant. By contrast, the addition of very acidic AC is rather detrimental. The addition of basic AC to Titania induces a substantial synergy effect by a factor up to 2.7 in the photoefficiency of the photocatalyst, suggesting that is possible to obtain clean water in a much shorter time than with TiO_2 alone. This synergism between both solids has been explained by an

important adsorption of the pollutants on AC followed by a mass transfer to photoactive TiO_2 through a common interface between AC and TiO_2. AC concentrates the initial pollutant and the degradation intermediate products enabling their transfer to TiO_2 and decomposition on it. Significant differences in intermediate product distributions were observed and ascribed to the different surface characteristics of AC indicating different mechanism of adsorption of the molecule and different reaction mechanism of oxidation as a function of the AC´s surface pH.

References

[1] Van Nostrand's Scientific Encyclopedia. Wiley-Interscience. John Wiley & Sons Inc; 9th Edition, Volume 2. New York, 2002.

[2] WHO 2002. Health in water resources development. *http://www.who.int/water sanitation_health/vector/water_resources.htm*

[3] D. M. Nevskaia, E. Castillejos-Lopez, Carbon 42 (2004) 653.

[4] WHO and UNICEF 2000. Global water supply and sanitation assessment 2000 report. *http://www.who.int/water_sanitation_health/Globassessment/GlobalTOC.htm*.

[5] S. B. Kim, H. T. Hwang, S. Ch. Hong, Chemosphere 48 (2002) 437.

[6] O. Legrini, E. Oliveros, A. M. Braun, Chemical Review (1993) 671.

[7] M.A. Fox and M. T. Dulay, Chemical Review, (1993) 341.

[8] D. F. Ollis, H. Al-Ekabi (Eds). Photocatalytic Purification and Treatment of Water and Air. Elsevier, Amsterdan, 1993.

[9] J. M. Herrmann, C. Guillard, P. Pichat, Catalysis Today 17 (1993) 17.

[10] O. Bannemann, J. Cunningham, M. A. Fox, E. Pelizzetti, P. Pichat, N. Serpone, in: G. R. Zepp, D. G. Crosby (Eds) Aquatic and Surface Photochemistry. Lewis, Boca Raton, 1994.

[11] D. M. Blake, Bibliography of work on the photocatalytic removal of hazardous compounds from Water an Air. NREL/TP-510-31319. NRE Laboratory Golden, Co, 2001.

[12] J. M. Herrmann, Catalysis Today 53 (1999) 115.

[13] W. Mu, J. M. Herrmann, P. Pichat, Catalysis Letter 3 (1989).

[14] J. M. Herrmann, J. Didier, P. Pichat, Chem. Phys. Letter 108 (1984) 618.

[15] J. F. Tanguay, S. L. Suib, R.W. Coughlin, J. Catalysis 117 (1989) 335.

[16] C. Minero, E. Catozzo, E. Pelizzetti, Langmuir 8 (1992) 489.

[17] N. Takeda, T. Torimoto, S. Sampath, S. Kuwabata, H. Yoneyama, J. Phys. Chem., 99 (1995) 9980.

[18] A. Bouzaza, A. Laplanche, J. Photochem. Photobiol. A: Chem., 150 (2002) 207.

[19] J. Matos, J. Laine, J. Brito, Appl. Catal. A: Gen., 152 (1997) 27.

[20] J. Matos, J. Laine, J. M. Herrmann, Carbon 37 (1999) 1870.

[21] J. M. Herrmann, J. Matos, J. Disdier, C. Guillard, J. Laine, S. Malato, J. Blanco, Catalysis Today 54 (1999) 255.

[22] J. Matos, J. Laine, J. M. Herrmann, J. Catalysis 200 (2001) 10.

[23] T. Torimoto, Y. Okawa, N. Takeda, H. Yoneyama, J. Photochem. Photobiol A: Chem., 103 (1997) 153.

[24] B. Tryba, A. W. Morawski, M. Inagaki, Appl. Catal. B: Environ., 41 (2003) 427.

[25] J. Arana, J. M. Rodriguez, E. Tello Rondon, C. Garrigahi Cabo, O. Gonzalez-Diaz, J.A. Herrera-Melian, J. Perez-Pena, G. Colon, J.A. Navio, Appl. Catal. B: Environ., 44 (2003) 161.

[26] J. Arana, J. M. Rodriguez, E. Tello Rondon, C. Garrigahi Cabo, O. Gonzalez-Diaz, J.A. Herrera-Melian, J. Perez-Pena, G. Colon, J.A. Navio, Appl. Catal. B: Environ. 44 (2003) 153.

[27] D. K. Lee, S. C. Kim, I. C. Cho, S. J. Kim, S. W. Kim, Separ. Purification Technol., 34 (2004) 59.
[28] C. H. Ao, S. C. Lee, J. Photochem. Photobiol. A: Chem., 161 (2004) 131.
[29] C. Leon, J. M Solar, V Calemma, L. R Radovic, Carbon 12 (1992) 797.
[30] G. Newcombe, R Hayes, M. Drikas, Colloids Surf. A., 11 (1995) 4386.
[31] M.V. Lopez-Ramon, F. Stoeckli, C. Moreno-Castilla, F. Carrasco-Marin, Carbon 37 (1999) 1215.
[32] G. Newcombe, R. Hayes, M. Drikas, Colloids Surf. A., 78 (1993) 65.
[33] P. Pichat, M. N. Mozzanega, J. Disdier, J. M. Herrmann, Nouv. J. Chim., 11 (1982) 559.
[34] A. Marinas, C. Guillard, J. M. Marinas, A. Fernandez, A. Aguera, Appl. Catal. B: Environ., 34 (2001) 241.
[35] A. Augün, Micro. Mesoporous Materials 66 (2003) 189.
[36] R.C Bansal, J.B Donnet, H.F Stoeckli, Active Carbon, New York, Decker (1988).
[37] M.L Studebaker, Rubber Chem. Technol., 39 (1957) 1400.
[38] T. J Fabish, D. E Schleifer, Carbon 22 (1984) 19.
[39] J. A Menendez, J. Phillips, B. Xia, L. R. Radovic, Langmuir 12 (1996) 4404.
[40] S. S Bartons, M. J. B Evans, E. Haliop, J. A. F. McDonald, Carbon 35 (1997) 1361.
[41] J. Matos, A. García, P. S. Poon, J. Mater. Sci., 45 (2010) 4934.
[42] J. Matos, M. Labady, A. Albornoz, J. Laine, J. L. Brito, J. Mater. Sci., 39 (2004) 3705.
[43] J. Matos, M. Labady, A. Albornoz, J. Laine, J. L. Brito, J. Molec. Catal. A: Chem., 228 (2005) 189.